Length-scales of mesoscale variability and eddies in the tropical South-East Atlantic Ocean based on satellite Altimetry observations

Issufo Halo[1,2,3], Roshin P. Raj[4,5], Anton Korosov[4], Mathieu Rouault[2], J. A. Johannessen[4,6], Pierrick Penven[7]

[1]Department of Conservation and Marine Sciences, Cape-Peninsula University of Technology,South-Africa
[2]Nansen-Tutu Centre for Marine Environmental Research, Dept of Oceanography, University of Cape Town, South-Africa
[3]Centre for Sustainable Oceans Economy, Cape-Peninsula University of Technology, South-Africa
[4]Nansen Environmental and Remote Sensing Centre, Bergen, Norway
[5]Bjerknes Center for Climate Research, Bergen, Norway
[6]Geophysical Institute, University of Bergen, Norway
[7]IRD, Plouzane, Brest, France

Mesoscale eddy occurrence and distribution in the tropical South-East Atlantic Ocean has been investigated using twenty-four years of satellite altimetry observations. Maps of absolute dynamic topography spatially gridded at ¼, on a daily basis were used covering a period between 1993 and 2017. The eddies spatial coverage has shown a significant equatorward decrease of their population, with increasing size. The cyclones and anticyclones exhibited similar Gaussian distribution, with no significant statistical difference between them, with predominant eddies having a radius of 70 km. Maps of horizontal length-scales of oceanic geostrophic flows, namely, the first baroclinic Rossby radius of deformation and the Rhine scales were inspected in order to explain the meridional distribution patterns of the eddy field. Both, the Rossby and the Rhine scales appeared to overlap to the north of 12°S, at about 100 km radius, in agreement with an early study which suggested an onset of a critical latitude in the region around 11.5°S. According to theories of 2D geostrophic turbulence these relations appear to explain the sharp equatorward transition of mesoscale regimes between nonlinear eddies and linear Rossby waves which are frequently observed in the region.

1. Introduction

As reviewed by Shillington et al. (2006), the main physical oceanographic processes in the South-East tropical Atlantic include the following: a dominant equatorward wind stress that induces coastal upwelling process along the coasts of South Africa and Namibia, instabilities of oceanic fronts, filaments, frontal jets, eastward/westward propagation of Kelvin/Rossby waves respectively (Koungue et al., 2017), internal waves (Ostrowski et al., 2009), and poleward propagation of coastal trapped waves along the Angolan coast (Rouault et al., 2007; Illig et al., 2019). Nevertheless, the oceanography of this region remains under studied, knowledge of the eddy occurrence and properties remains scanty, even though eddies are important geophysical structures in the region, capable to shape the ocean biology, and the climate variability and predictability. To complement the existing knowledge, in this study we have investigated the eddy occurrence and their distribution by assessing the horizontal length scales of mesoscale geostrophic flow variability inferred from the relation between the first baroclinic Rossby radius of deformation and the Rhines scale.

2. Data and Methods

The data used to map the first baroclinic Rossby radius of deformation in this study was derived from The global dataset published by Chelton et al. (1998), which is computed using the equation:

$$RD = \int_{-h}^{0} \frac{N}{|f|\pi} dz \qquad (1)$$

Where N is the Brunt-Vaisala stratification frequency, h is oceanic depth level, and f is Coriolis parameter. The Rhines scale L_R was determined following Rhines (1975), using the equation

$$LR = \sqrt{\frac{Urms}{2\beta}} \qquad (2)$$

Where U_{rms} is the eddy's rotational speed, estimated from eddy kinetic energy $EKE = \frac{u'+v'}{2}$, using the relation, $U_{rms} = 2EKE$.
The EKE was calculated using the fluctuations of the horizontal components of the geostrophic velocities u' and v', determined from maps of the absolute dynamic topography, measured by satellite altimetry. The data is gridded at ¼ in longitude and latitude, on a daily timescale, and the period used here spans from 1993 to

2017. The data is freely available at Copernicus Marine Environmental Services (CMEMS).

The eddies were extracted from the eddy field tracked by Halo et al., [submitted]. The equivalent eddy mean radius R was estimated using the relatio proposed by Souza et al. (2011).

$$R = \sqrt{\frac{\sum A}{N\pi}} \qquad (3)$$

Where A is the eddy's surface area, assumed to have a circular geometry, and N is the total number of eddies.

3. Results

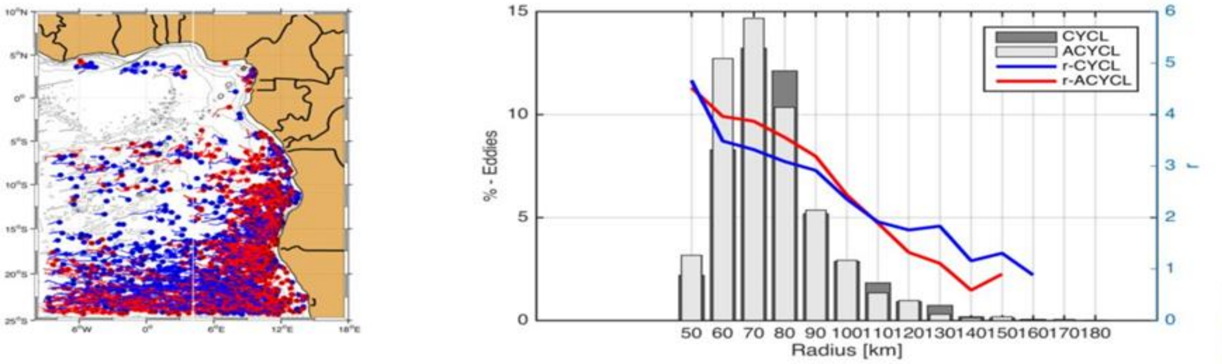

Figure 1: a) Eddy generation sites and eddies trajectories, determined from an automatic eddy detection and tracking algorithm applied on altimetric maps of absolute dynamic topography, from 1 January 1993 to 31 December 2017, for eddies with a lifespan of 7 days and longer. Red dots (anticyclones) and blue (cyclones), with the background contours representing the seafloor topography. b) Eddy size distribution (% of occurrence, in radius clustered between 50 km and 170km at every 10 km interval). Dark grey (cyclones) and light grey (anticyclones) for the eddies determined in the tropical South-East Atlantic Basin. The overlay lines represent eddy non-linearity parameter (r), for cyclones (blue), and anticyclones (red), from Halo et al. [submitted].

Figure 1a shows the spatial distribution of the eddy generation sites and the eddies trajectories. Only eddies with a lifespan of 7 days and greater were selected. Blue dots represent cyclonic, and red represents anticyclonic eddies. The statistics performed by Halo et al [submitted], suggests that a total of 1642 eddies are present in Figure 1a. This corresponds to 52.3% anticyclonic (red) and 47.7% cyclonic (blue). The result also suggests that there are more eddies being formed in the southern parts than in the northern parts of the domain. The generation of eddies in the vicinities of the continental shelf in the northern sector (between 5ºN S and 2ºN) (Figure 1a) resembles coastally trapped eddies documented by Djakoure et al. (2014) in the Gulf of Guinea. Results from their numerical model simulation have indicated that these eddies are formed mostly by mean of flow interactions and barotropic instabilities associated with the Cape Palmas and Cape Three-Points, located to the western and eastern of Ivory Coast respectively (Djakoure et al., 2014). Nevertheless, they fall outside of our region of interest, thus are not investigated further in the present study. On the other hand, the generation of the eddies in the southern sector, supports the hypothesis presented by Colberg and Reason (2007), which suggests the prevalence of eddies across the Angola Benguela Frontal Zone, as also documented by Meeuwis and Lutjeharms (1990). The latter attributed to frontal instabilities as the driving physical mechanism responsible for their formation. Figure 1b shows the histograms of their density distribution, expressed in terms of frequency of occurrences in %, as function of eddies radii in km. The eddies have been clustered between radius of 50 and 170 km, at every 10 km. The dark gray (light gray) shadings represent cyclonic (anticyclonic) eddies respectively (Figure 1b). Both exhibit similar distribution (e.g. Gaussian), with peak cantered at 70 km radius, which suggest that they are generated mostly by the same physical processes. The blue and red colour super-imposed in Figure 1b, represent the non-linearity parameter *(r)* for the cyclonic and anticyclonic eddies respectively. The r has been determined following the metric ratio between the eddy's rotational velocity (U_{rms}) against its translational speed c, expressed as $r=U_{rms}/c$, as proposed by chelton et al. (2007). When this relation yields to a r that is greater than 1 (i.e. r>1), it is assumed that the rotational velocities are stronger than the translation speed, thus implying that the eddies are non-linear and non-dispersive, with potential to trap materials in their cores. An interesting pattern observed in Figure 1b is that r decreases consistently with increasing radius. As discussed in Halo et al. [submitted], Theiss (2004) computed an equivalent r, using the relation between the first baroclinic Rossby radius of deformation (R_D) and Rhine scale (L_R), whereby $r=R_D/L_R$). He demonstrated that for $r>1$ the waves do not transfer energy into zonal flows, permitting the emergence of eddies. Whereas for $r<1$ the waves dissipate into zonal alternating flows (Theiss, 2004). Halo et al [submitted] demonstrated that in this region a critical latitude value corresponding for $r=1$ is achieved at about 11.5°S. This is further corroborated in Figure 2, where the relationship between R_D, L_R can be inferred by comparing Figure 2a against Figure 2b respectively.

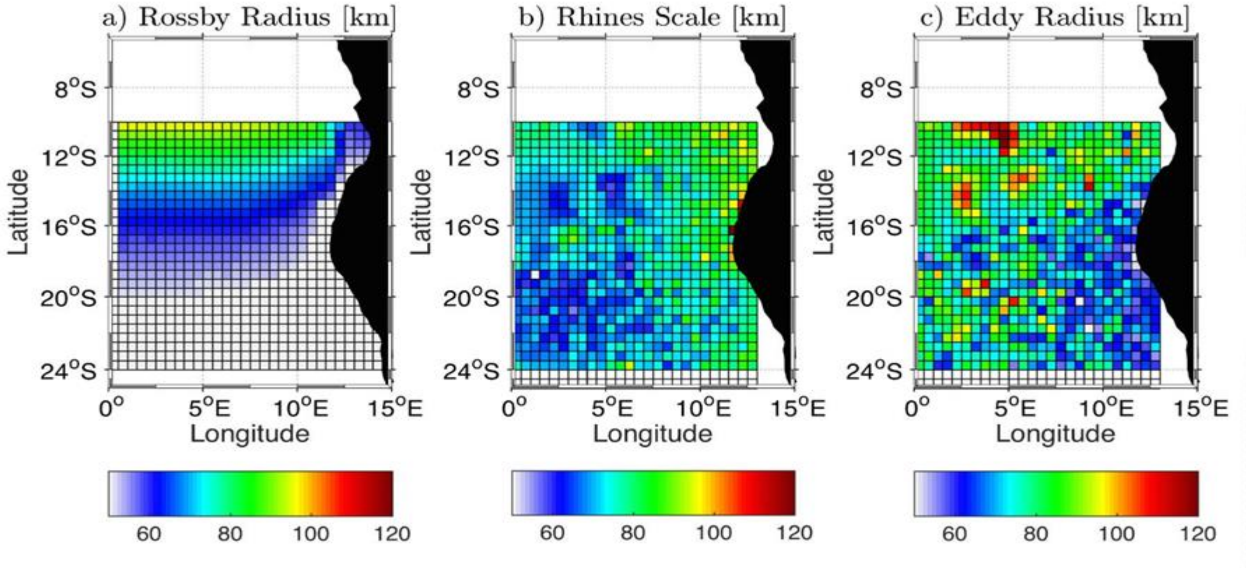

Figure 2: Spatial distribution of the horizontal length-scales of geostrophic flows, a) first baroclinic Rossby radius of deformation from Chelton et al. (1998), determined from equation 1, b) Rhine scale, determined from equation 2, and c) radii of the tracked eddies, estimated with equation 3.

It is evident that an overlap of the length scales occurs only to the north of 12°S, which supports the onset of critical latitude towards 11.5°S. In Figure 2c, R represents the eddy radius. Notice that it is towards this latitudinal band that a maximum eddy size is achieved (Figure 2c). Overall in Figure 2, it is notable that all these length scales grow equatorward. R_D ranges from 40 km in the south to 150 km in the north. L_R ranged between 80 km and 120 km without a specific spatial pattern, and R between 60 km and 120 km, with a relatively clearer spatial distribution than L_R, with its lower ranges more in the south and upper ranges more in the north. Also it is evident that R grows zonally from the coast towards off-shore (Figure 2c).

4. Conclusions

In this study we have demonstrated that mesoscale eddies are present in the tropical South-East Atlantic Ocean. They are more prevalent in the Cape Basin than in the Angola Basin, indicating an equatorward decrease of their population. Both cyclonic and anticyclonic showed similar near Gaussian distribution, and had almost the same prevalence, 52% (anticyclones) and 48% (cyclonic). Their maximum sizes were predominantly observed to the north of 12°S, where R_D and L_R overlaps, allowing for the determination of a critical latitude band, whereby the theories of 2D geostrophic turbulence would favour regime transition between nonlinear eddies and linear waves. This may explain why there are fewer eddies to the north of 12°S, when compared to other regions of the world oceans.

References

Chelton, D. B., R. A. deSzoeke, M. G. Schlax, K. El Naggar, and N. Siwertz (1998), Geographical variability of the first-baroclinic rossby radius of deformation. J. Phys. Oceanogr., 28:433– 460.

Chelton, D. B., M. G. Schlax, R. M. Samelson, and R. A. Szoeke (2007), Global observations of large oceanic eddies. Geophys. Res. Lett., 34: L15606, 2007. doi:10.1029/2007GL030812.

Colberg, F., and J. C. Reason (2007), A model investigation of internal variability in the Angola Benguela Frontal Zone. J. Geophys. Res., 112:C07008. doi: 10.1029/2006JC003920.

Djakoure, S., P. Penven., B. Bourles., J. Veitch, and V. Kone (2014), Coastally trapped eddies in the north of the Gulf of Guinea. J. Geophys. Res., 119:6805-6819. doi: 10.1002/2014JC010243.Halo, I., Roshin. P. Raj, A. Korosov, P. Penven, M. Mathieu, and J. A. Johanessen. Mesoscale variability, critical latitude and eddy mean properties in the tropical South-East Atlantic Ocean. J. Geophys. Res., [submitted].

Illig, S., and M-L. Bachelery (2019), Propagation of Subseasonal Equatorially Force Coastal Trapped Waves down to the Benguela Upwelling System. Nature Sci Rep.,9:5306. doi: 10.1038/s41598-019-41847-1.

Kongue, R. A. I., S. Illig, and M. Rouault (2017), Role of interannual Kelvin wave propagations in the equatorial Atlantic on the Angola Benguela Current system. J. Geophys. Res., 122:4685-4703. doi: 10.10002/2016JC012463.

Meeuwis, J. M., and J. R. E. Lutjeharms (1990), Surface thermal characteristics of the angola-benguela front. Afr. J. mar. Sci., 9:261-279.

Rhines, P. B (1975), Waves and turbulence on a β plane. J. Fluid Mech., 69:417-443.

Rouault, M., S. Illing, C. Bartholomae, C. J. Reason, and A. Bentamy (2007), Propagation and origin of warm anomalies in the Angola Benguela upwelling system in 2001. J. Mar. Sys. doi: 10.16/j.jmarsys.

Shillington, F. A., C. J. C. Reason, C. M. Duncombe Rae, P. Florenchie, and P. Penven (2006), Large scale physical variability of the Benguela Current Large Marine Ecosystem (BCLME). In V. Shannon, G. Hempel, P. Malanotte-Rizzoli, C. Moloney, and J. Woods, editors, Large Marine Ecosystems: The Benguela: predicting a large marine ecosystem, volume 14, pages 4768. Elsevier, Amsterdam.

Souza, J. M. A. C., C. de Boyer Montegut, and P. Y. Le Traon (2011), Comparison between three implementations of automatic identication algorithms for the qualication and characterization of mesoscale eddies in the South Atlantic Ocean. Ocean Sci, 7:317-334. doi:10.5194/os-7-317-2011.

Theiss, J (2004), Equatorward energy cascade, critical latitude, and the predominance of cyclonic vortices in geostrophic turbulence. J. Phys. Oceanogr., 34:1663-167